Aging Cell (2010) **9,** pp383–397 Doi: 10.1111/j.1474-9726.2010.00568.x

The load of short telomeres, estimated by a new method, Universal STELA, correlates with number of senescent cells

Laila Bendix,[1,2,3] Peer Bendix Horn,[4] Uffe Birk Jensen,[5] Ivica Rubelj[6] and Steen Kolvraa[1,2,7]

[1]Danish Aging Research Center (DARC), University of Southern Denmark, Odense, Denmark
[2]Department of Clinical Genetics, Vejle Hospital, Vejle, Denmark
[3]Department of Public Health, University of Copenhagen, Copenhagen, Denmark
[4]Department of Clinical Biochemistry, Vejle Hospital, Vejle, Denmark
[5]Department of Clinical Genetics, Aarhus University Hospital, Aarhus, Denmark
[6]Ruder Boskovic Institute, Zagreb, Croatia
[7]University of Southern Denmark, Regional Institute for Health Sciences, Odense, Denmark

Summary

Short telomeres are thought to trigger senescence, most likely through a single – or a group of few – critically shortened telomeres. Such short telomeres are thought to result from a combination of gradual linear shortening resulting from the end replication problem, reflecting the division history of the cell, superimposed by a more stochastic mechanism, suddenly causing a significant shortening of a single telomere. Previously, studies that have tried to explore the role of critically shortened telomeres have been hampered by methodological problems. With the method presented here, Universal STELA, we have a tool that can directly investigate the relationship between senescence and the load of short telomeres. The method is a variant of the chromosome-specific STELA method but has the advantage that it can demonstrate short telomeres regardless of chromosome. With Universal STELA, we find a strong correlation between the load of short telomeres and cellular senescence. Further we show that the load of short telomeres is higher in senescent cells compared to proliferating cells at the same passage, offering an explanation of premature cell senescence. This new method, Universal STELA, offers some advantages compared to existing methods and can be used to explore many of the unanswered questions in telomere biology including the role that telomeres play in cancer and aging.

Key words: abrupt shortening; aging; cancer; polymerase chain reaction; senescence; telomere.

Introduction

The fact that telomeres shorten gradually by each cell division was shown almost 20 years ago by Harley *et al.*, (1990), closely connecting telomeres to the aging of the cell. It had been hypothesized that this shortening of telomeres would occur as a result of the end replication problem (Olovnikov, 1973), but it was realized early on that the shortening rate of telomeres exceeded what could be predicted by this mechanism. Later studies have found that the shortening is a highly controlled process exploiting exonucleases, shortening not only the lagging, but also the leading strand (Sfeir *et al.*, 2005).

The shortening of mean telomere length was found to correlate not only with cell age, but also with the replication potential of the cell (Allsopp *et al.*, 1992; Allsopp & Harley, 1995) as well as with donor age in various tissue types (Hastie *et al.*, 1990; Lindsey *et al.*, 1991; Bischoff *et al.*, 2005; Alter *et al.*, 2007). Short telomeres are thought to be a mediator of senescence, triggering the DNA damage response leading to a G1/S cell cycle arrest (d'Adda di Fagagna *et al.*, 2003), although there is a general agreement that also nontelomere-dependent senescence inducing mechanisms exist (culture conditions, mutations in oncogenes, chromatin perturbation) (Sherr & DePinho, 2000; Parrinello *et al.*, 2003; Passos & Von Zglinicki, 2006). The major role of short telomeres in senescence is supported by the fact that expression of telomerase, the telomere elongating enzyme complex, can circumvent senescence (Bodnar *et al.*, 1998).

A number of observations have, however, questioned a causal link between the gradual decrease in general telomere length and senescence induction. First of all, the induction of senescence seems to be bimodal and with an increasing proportion of cells entering senescence at late passages (Smith & Whitney, 1980), while mean telomere length seems to shorten in an almost linear fashion (Counter *et al.*, 1992; Levy *et al.*, 1992; Vaziri *et al.*, 1994; Henderson *et al.*, 1996). Secondly, in tissue cultures senescence was found to be induced with a mean telomere length much longer than what would be expected to trigger the senescence mechanisms.

Based on these findings, a number of groups have suggested that telomere-associated senescence may instead be triggered

Correspondence
Laila Bendix, Hans Appels Vej 14, DK-5260 Odense S, Denmark.
Tel.: +45 2615 6501; fax: +45 7940 6871; e-mail: laila.bendix@slb.regionsyddanmark.dk, laila.bendix@dadlnet.dk
The work was carried out at:
Department of Clinical Genetics, Laboratory Center, Vejle Hospital, Kabbeltoft 25, DK-7100 Vejle, Denmark

Accepted for publication 16 *February 2010*

Aging Cell

by a single – or a group of few – short telomeres within the cell (Hemann *et al.*, 2001; Zou *et al.*, 2004; Abdallah *et al.*, 2009) and not necessarily by a global decrease in telomere length. Such short telomeres are known to be consistently present in cell samples as a normal phenomenon and is believed to be a reflection of the fact that telomeres from different chromosome arms differ in length in a specific manner (Martens *et al.*, 1998; Graakjaer *et al.*, 2003) in combination with different cells in a sample having gone through a different number of cell divisions.

The single very short telomeres that are sometimes seen when analyzing cells with relatively long mean telomere length, e.g. as signal free ends in metaphase fluorescence insitu hybridization (FISH) or as a single ultra-short telomere with STELA (Martens *et al.*, 2000; Baird *et al.*, 2003), can, however, not be fully explained by replication-driven telomere shortening alone. These short telomeres must instead have been formed by a sudden loss of a large telomere fraction from that particular telomere. Different mechanisms for such a shortening of telomeres have been suggested, among others oxidative damage inflicting single-strand breaks in the telomeres (Von Zglinicki *et al.*, 1995; Passos *et al.*, 2007; Richter & von Zglinicki, 2007), replication slippage and unequal sister-chromatid-exchange (Baird *et al.*, 1995; Baird, 2008), and recombination causing circularization and thus deletion of distal repeats (Rubelj & Vondracek, 1999; Rubelj *et al.*, 2002; Wang *et al.*, 2004; Ferenac *et al.*, 2005).

Based on these observations, it is therefore at present the general believe that telomeres are shortened by a combination of gradual linear shortening resulting from the end replication problem and postreplicative modifications, reflecting the number of cell divisions, superimposed by a more stochastic mechanism, suddenly causing an extensive shortening of a single telomere. Over time, a combination of these two shortening mechanisms is believed to result in a more random occurrence of single, critically shortened telomeres with the potential to trigger early senescence response as cell proliferation proceeds.

A number of research groups have tried to obtain experimental evidence for a role of single, short telomeres in the triggering of cellular senescence. Much of this evidence has, however, been either indirect or acquired through manipulation of cellular systems (Abdallah *et al.*, 2009). A few groups have, however, used a more direct approach for studying the relationship between telomere length and senescence by characterizing telomere length distribution on cell fractions that had been flow sorted into senescent and proliferating populations (Martin-Ruiz *et al.*, 2004; Ferenac *et al.*, 2005). In such experiments, the Von Zglinicki group found that, in normal fibroblast cultures, subpopulations of senescent cells had shorter telomeres than subpopulations of proliferating cells, mainly attributed to the senescent population having a larger fraction of shorter telomeres evaluated by telomere restriction fragment length assay (TRF). The Rubelj group, on the other hand, found no difference in mean telomere length between proliferating and senescent populations.

For both groups, conclusions are based mainly on data obtained by the TRF (Allshire *et al.*, 1989; Allsopp *et al.*, 1995). This is a limitation because this assay measures mainly mean length of telomeres and is not optimal for measuring short telomeres. A few groups have had some success extracting information on the shortest telomeres by detailed analysis of TRF smears (Kimura *et al.*, 2008a), but the general feeling is that the assay is biased against the shorter telomeres.

Only few other methods posses the ability to measure short telomeres more precisely. Of the different Q-FISH-based techniques available, the version applied to metaphases (Lansdorp *et al.*, 1996; Graakjaer *et al.*, 2003) seems best suited for visualizing rare, very short telomeres. This method is, however, limited to material containing live, dividing cells, excluding studies of senescent cells. Even though the other Q-FISH methods [Flow (Rufer *et al.*, 1998), interphase (O'Sullivan *et al.*, 2004), and HT (Canela *et al.*, 2007)] allow the quantification of percentage of cells with short mean telomere length, a single short telomere within a cell with long mean length will not be detected with these methods.

The single telomere length analysis, STELA, which is a ligation-PCR-based method (Baird *et al.*, 2003), seems at present the most suitable method for measuring short telomeres. Its limitation is, however, that it can only be applied to a few chromosomes, because of the need for designing chromosome-specific proximal primers (Britt-Compton *et al.*, 2006), which limits its use when studying the distribution and role of critically short, single telomeres in senescent cells.

It could in this context be argued that it would be sufficient to study the changes at one, or a few, single telomeres to get an unbiased picture of the distribution of short telomeres in general. Such an argument would, however, be based on the assumption that sudden changes in telomere length would occur with the same frequency on all chromosome ends, i.e., changes similar to those seen at the XpYp telomeres would also occur at all other telomeres, and to the same extent, making XpYp STELA measurements a useful surrogate measure for all other chromosome ends. Knowing that there is a substantial difference in telomere length within a cell, the longest telomere being on average approximately 70% longer than the shortest in dividing cells (Graakjaer *et al.*, 2003), it could, however, be hypothesized that telomeres from certain chromosomes would be more commonly represented among the critically short telomeres. For a time, it was even believed that a specific chromosome was 'programmed' to be responsible for the induction of senescence [17p has been suggested (Martens *et al.*, 1998)]. The current believe is, however, that any chromosome end with an ultra-short telomere can induce senescence, but it is still unclear whether certain chromosome ends are carrying critically short telomeres more frequently than other chromosome ends and therefore are more common mediators of telomere-driven senescence.

Our aim in this study was therefore to develop a method, better suited for measuring short telomeres in a cell sample, and validate it in cell culture systems. The method we developed, named Universal STELA, is a variant of the original STELA method. Contrary to the original STELA, it is able to measure the

load of the short telomeres in a biological sample regardless of on which chromosome end, the short telomere is located. We will first present the principles and validation of the method and subsequently present results showing how the load of short telomeres, as estimated by this method, correlates strongly with SA-β-Gal staining, as well as how short telomeres are more abundant in senescent subpopulations than in cycling subpopulations in a population of cells from the same passage.

Method development and validation

Basic features

The new feature of Universal STELA, compared to the original STELA, is the use of a second ligation-based step. The principle of the method is as follows: extracted DNA is digested by restriction enzymes, leaving a sticky overhang of the proximal end of the telomere-containing fragments. A double-stranded oligo with one overhang complementary to the digested DNA is then annealed and ligated to the overhang created by the restriction enzyme. The other end of the double-stranded oligo is designed, so that the DNA fragments are tagged with a noncomplementary tail, to which a PCR primer can be designed. A distal primer sequence is added to telomeric fragments as in the original STELA (Baird *et al.*, 2003) by annealing a linker, telorette, to the G-rich 3′-overhang of the telomeres and ligating it to the 5′-end of the complementary C-rich strand. In this way, the distal ends of telomere-containing fragments are tagged with a unique sequence to which another PCR primer can be designed.

To preferentially amplify the telomeric ends, the proximal double-stranded oligo has been designed in such a way that a fragment would form a panhandle loop if the proximal base-paired oligos are present at both ends of the DNA fragment. This technique is known as suppression PCR (Lavrentieva *et al.*, 1999) and will suppress PCR products from intragenomic fragments that have base-paired oligos in both ends without hampering the efficiency of the desired PCR of telomere-containing fragments. (For a detailed explanation and oligo sequences see Fig. 1 and Table 1).

As shown with the chromosome-specific STELA, PCR products representing telomeric fragments are seen as a multitude of discrete bands, where each band is believed to represent the length of one single telomere block (Fig. 2A lanes 2–5). Because of the heterogeneity of telomere length, it must be expected that even very small samples of DNA will contain telomere blocks of many different lengths as also clearly demonstrated by Baird *et al.* (2003). Therefore, nine PCRs are performed in one analysis to achieve a proper representation of the short telomeres present in the sample, an approach also taken by others using single chromosome STELA (Baird *et al.*, 2003; Sfeir *et al.*, 2005).

Digestion

The initial digestion step is carried out with a mix of two restriction enzymes leaving the same sticky overhang. The choice of enzyme is as important to the result of Universal STELA, as it is to TRF assays (Baird *et al.*, 2006), because the restriction enzyme determines the size of the subtelomeric fragment that will be included in the estimated telomere length. To minimize the size of this subtelomeric fragment, we measured mean telomere length by TRF assay after digesting the genomic DNA with a number of different enzyme combinations. In this series of experiments, it became clear, as also shown by others, that enzymes recognizing variant telomeric repeats gave the shortest mean telomere length (Baird *et al.*, 1995; Kimura *et al.*, 2008b). Such variant or imperfect repeats are located very proximal in the telomere block or immediately adjacent to the telomeric block. The imperfect repeats are most likely arising from replication slippage or an occasional base substitution (Baird *et al.*, 1995).

The combination of MnlI and HphI, both of which cut variant repeats, gave a TRF mean telomeric length more than 1 Kb shorter than the traditionally used HinfI/RsaI mixture. We had, however, to discharge MnlI/HphI in Universal STELA, mainly because of the overhang including an N, making the sticky end less suitable for the subsequent ligation. Instead, we chose MseI as the primary cutter, because this enzyme recognizes the sequence TTAA which was found to be quite frequent in the sequenced subtelomeric regions (NCBI Build 35.1). The TTAA sequence will arise as a part of the telomeric repeat variant TTAAGGG, which in general seems to be a less common variant repeat (Baird *et al.*, 1995; Riethman, 2008). A TRF assay with MseI gave a mean telomere length value only 0.4 Kb longer than MnlI/HphI. In the digestion, we furthermore included NdeI, because the addition of this rather frequent cutter generates shorter intragenomic fragments, which increases the panhandle inhibition as well as cuts some of the subtelomeric regions.

It should be mentioned that for those chromosomes where the subtelomeric sequence is known, we were able to demonstrate that in combination MseI and NdeI restriction sites were at a mean distance of < 300 bp (range 20–1810 bp) from the perfect telomeric repeats (NCBI Build 35.1).

After digestion with MseI/NdeI, we obtained no telomeric PCR products with the original XpYp STELA (data not shown), as expected, because the subtelomeric sequence of XpYp contains an MseI/NdeI recognition site distal to the site used for priming (344 bp distal to the telomeric tract).

The overall conclusion of the digestion experiments is that the MseI/NdeI mixture digests the DNA very close to or very proximal in the telomeric block, leaving at worst only a very short, although unknown, part of nonperfect telomeric or nontelomeric DNA in our final PCR product or possibly, but rarely cutting the telomere in the most centromeric part of the telomeric repeat block.

Linker oligos and primers

Ligation of the panhandle oligo was documented to be successful, because both the digestion to create the sticky overhang and the presence of base-paired double-oligos are necessary to

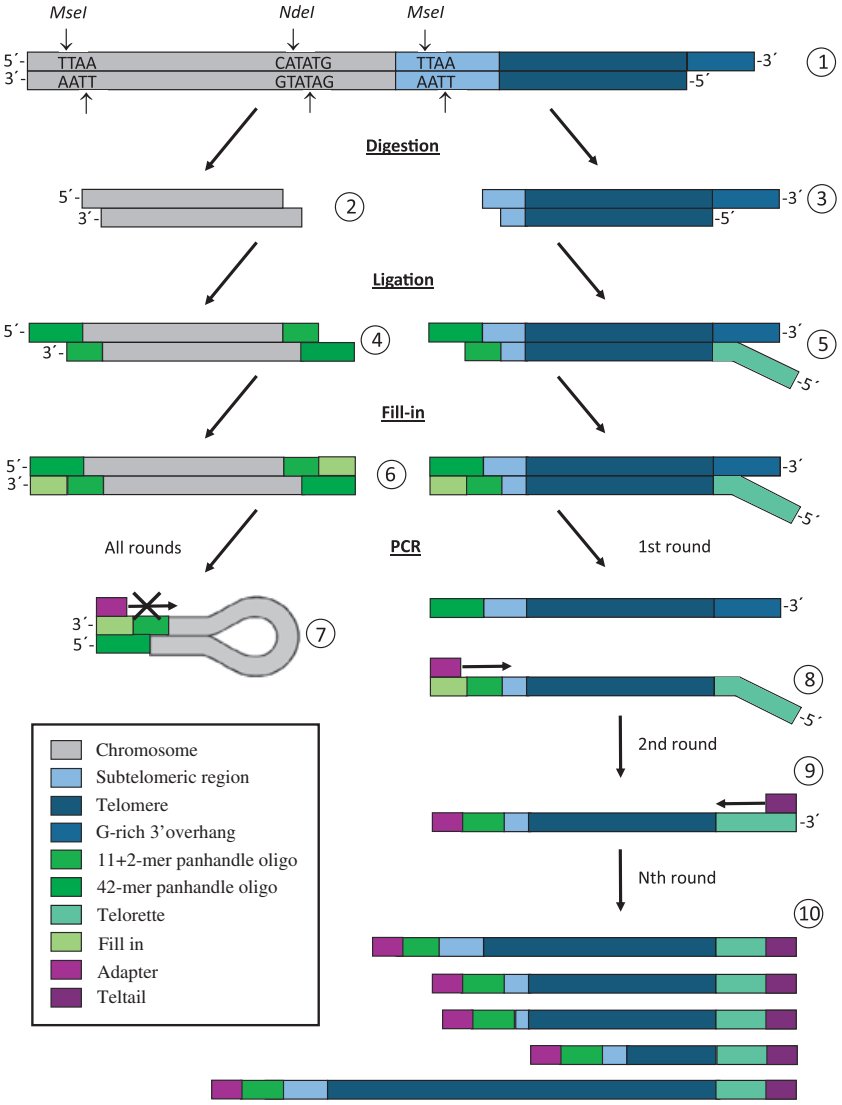

Fig. 1 Universal STELA assay principles. Extracted DNA is digested by restriction enzymes MseI/NdeI (1). The digestion mainly generates pieces of genomic DNA of 10–3000 bp, the great majority of which has the same sticky overhang 5′-AT-3′ at both ends (2). However, for every chromosome end a fragment of DNA with the telomeric region including the 3′-overhang at one end and a smaller part of the subtelomeric region with a 5′-AT-3′ overhang at the other end, is also formed (3). The next step is a ligation-based step, in which two specially designed oligos (42-mer and 11 + 2-mer panhandle oligo) are annealed and ligated to the proximal overhang and to both ends of non-telomeric fragments (for oligo sequences see Table 1). These two oligos are designed so that they spontaneously anneal, forming a two-base sticky overhang complementary to the overhang formed by the digestion. The other end of the paired oligos is a long, single-stranded and GC-rich overhang (4 and 5). The third step is another ligation step. An oligo (telorette) is annealed to the G-rich 3′-overhang of the telomeric repeat (5). This oligo consists of seven bases complementary to the telomere repeat sequence and a tail of 20 non-complementary nucleotides. After annealing the telorette is ligated to the 5′- end of the C-rich strand of the telomere. Finally a fill-in step is required (6) so that the GC-rich proximal overhang becomes double stranded, hereby serving as template for the upstream PCR primer (the adapter primer). In the first step of the PCR all DNA pieces are denatured. When the temperature is lowered for the annealing step, two things can happen. For the intra-genomic fragments where the upstream sequence isligated to both ends, the complementary ends will anneal to each other, forming a panhandle, which will be relatively stable due to a high melting temperature of the panhandle sequence. A PCR, based on intragenomic fragments as template, will therefore be suppressed (7). For the telomeric fragments (8), the adapter will anneal to the filled-in part of the upstream sequence, thereby initiating PCR. In the following PCR cycles the teltail primer will be able to anneal to the PCR product obtained by the adapter primer (9), thereby producing telomeric products of different lengths reflecting the lengths of the individual telomeres (10).

produce a PCR product (Fig. 2A lane 7–8 and 9–10, respectively). Ligation of the telorette is an established method (Baird *et al.*, 2003), which is also accomplished under our modified conditions. This step is necessary as no PCR product is achieved if (i) the telorette is excluded, (ii) no ligase is added, or (iii) the 3′-overhang is digested prior to ligation by mung bean endonucleases (Fig. 2A lane 11–12, 13–14 and 15–16, respectively).

Because we do not try to remove panhandle oligos or the telorette oligo prior to PCR, these might theoretically work as primers. It would in this connection be a concern if the 3′-end of the telorette could initiate PCR cycles as this could happen randomly on the telomeric tract, resulting in truncated products. The Tm of the telomere complementary 3′-end of the telorette is, however, more than 30 °C lower than the Tm of the teltail oligo

Table 1 Oligos and primers used for XpYp STELA and Universal STELA

Oligos specific for Universal STELA	Sequence
11 + 2-mer - panhandle	5′-TAC CCG CGT CCG C - 3′
42-mer - panhandle	5′- TGT AGC GTG AAG ACG ACA GAA AGG GCG TGG TGC GGA CGC GGG - 3′
Adapter	5′- TGT AGC GTG AAG ACG ACA GAA - 3′
Oligos specific for XpYp STELA	**Sequence**
XpYpE2	5′- TTG TCT CAG GGT CCT AGT G -3′
Common oligos	**Sequence**
Telorette 1	5′- TGC TCC GTG CAT CTG GCA TCC CCT AAC- 3′
Telorette 2	5′- TGC TCC GTG CAT CTG GCA TCT AAC CCT- 3′
Telorette 3	5′- TGC TCC GTG CAT CTG GCA TCC CTA ACC- 3′
Telorette 4	5′- TGC TCC GTG CAT CTG GCA TCC TAA CCC- 3′
Telorette 5	5′- TGC TCC GTG CAT CTG GCA TCA ACC CTA- 3′
Telorette 6	5′-TGC TCC GTG CAT CTG GCA TCA CCC TAA- 3′
Teltail	5′-TGC TCC GTG CAT CTG GCA TC - 3′ -DIG
Telomere-probe	$(TTAGGG)_7$ - DIG

used for PCR. Therefore, priming from annealed telorette oligos is very unlikely to happen under the chosen PCR conditions. Furthermore, the concentration of the telorette is 10^4-fold lower than the primer concentration. In repeated experiments, we found that the teltail primer is necessary to achieve any PCR product, supporting the perception that the telorette does not function as a PCR primer itself (Fig. 2A lanes 17–18).

Concerning the 42-mer oligo involved in the panhandle formation, we have found that when adding high amounts of template mix, a few discrete bands are seen, even when the adapter primer is omitted. This is most likely attributed to the relatively high concentration of the 42-mer oligo. We are, however, of the opinion that this priming is of minor importance for two reasons. Firstly, no products are obtained if the panhandle oligos are not successfully ligated (Fig. 2A lane 7–10), suggesting that they do not mis-prime to other genomic templates. Secondly, we have shown that it is the adapter primer that is active in the PCR (Fig. 2C).

It could also be a concern that the presence of the linker oligos could hamper the efficiency of the PCR, and therefore we performed experiments where both panhandle oligos and the telorette oligo had been removed before the PCR. In these experiments, we observed no increase in PCR efficiency by this purification (data not shown). In a separate experiment, we also investigated whether the use of up-stream linker oligos causing panhandle formation gave higher PCR efficiency than linker oligos without sequences causing panhandle formation. Here, it was found that the inclusion of panhandle-sequences substantially improves the efficiency of the PCR (data not shown).

Template amount

In general, the PCR needs very small amounts of template DNA, which is one of the major advantages of this method. But it is also an aspect to which one has to pay great attention. In Fig. 2B, the influence of different amounts of template is shown. It is seen how the banding pattern achieved with Universal STELA depends strongly on the amount of template DNA. The general trend is that discrete bands occur only when the amount of template DNA is below 100 pg. When exceeding this amount of template per reaction, bands begin to form a smear, increasing the risk of obtaining truncated telomeric products. To avoid this, we recommend that 10–40 pg template per reaction is used for Universal STELA PCR.

Product characterization

Some of the very short bands seen on the gels might theoretically have been derived from amplification of short intragenomic sequences harboring telomere-like repeats which had escaped the panhandle suppression. An experiment (See Fig. 2C) was therefore designed to verify that the products visualized on the blot were in fact representing true telomeric ends. The fact that no bands were found in Lanes B and D in Fig. 2C indicates that one end of even the very short fragment initially contained the overhang generated by restriction enzyme digestion at one end and the other end contained the 3′-single-stranded telomeric overhang which was subsequently ligated to the telorette. These findings indicate that all bands in the gel – including the very short bands – were derived from telomere blocks located at chromosome ends.

The load of short telomeres

Universal STELA was developed to estimate the load of critically short telomeres in a cell. When working with chromosome-specific STELA, most authors have chosen to describe the state of the telomeres by the mean length of fragments obtained by the STELA reaction. Given that senescence is believed to be induced by telomeres activating the DNA damage response when they are shortened below a certain critical length, the relevant parameter to use, when wanting to correlate telomere length with senescence, would from a logical point of view be the number of such critically shortened telomeres per single cell. To use this measure, we must, however, first set a threshold for when telomeres are critically shortened. Data have suggested that in normal fibroblasts, the threshold is 1–2 kb (Martens *et al.*, 2000). During development of the assay, we have applied different thresholds between 500 and 2000 bp. From this explorative work, a threshold of 1500 bp seems preferable. The parameter when applying the Universal STELA method is therefore the number of telomeres obtained below a threshold of 1500 bp per genome equivalent template, i.e. for every 8 pg of DNA used for the PCR (load of short telomeres). The applicability of this approach will be shown in the result section below.

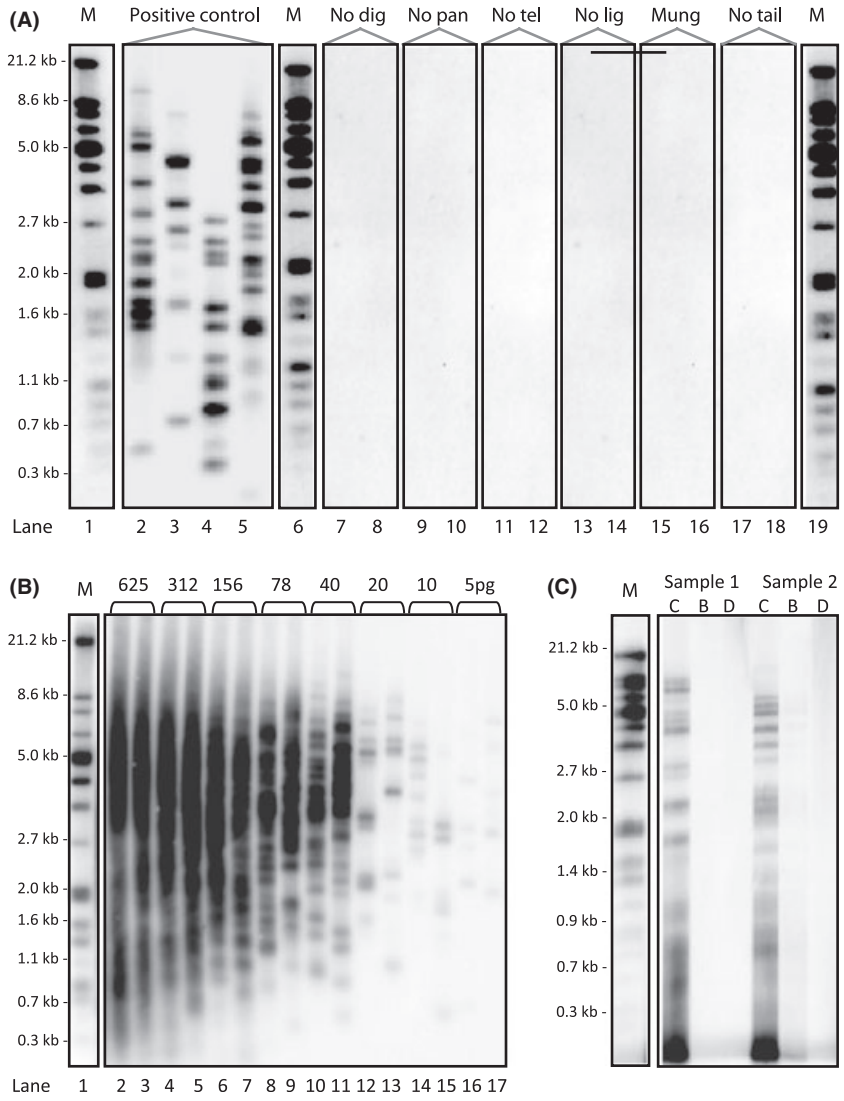

Fig. 2 Validation of Universal STELA. A: A PCR product is not produced, when the DNA is not digested (no dig: No digestion due to no restriction enzymes added (lane 7–8)), or when no panhandle or telorette is ligated to the digested DNA (no pan: the two panhandle oligos are not added in the first ligation step (lane 9–10); no tel: a telorette is not added in the second ligation step (lane 11–12)). Neither does a product appear when the ligase is omitted (no lig: lane 13–14), when the 3′-overhang is digested prior to ligation with mung bean endonuclease (mung: lane 15–16) or when the teltail primer is omitted (no tel: lane 17–18). B: Sensitivity of Universal STELA by serial dilution of template (5–625 pg). Universal STELA is very sensitive to the amount of template used. When using too high amounts of template (> 100 pg) a smear is seen. We believe this represents unfinished PCR products working as primers that cause a network of artifactproducts of many different lengths. C: Control of PCR products based on retention with magnetic beads. A large volume (25 μL) of Universal STELA PCR mix was obtained using a teltail-primer tagged with digoxigenin and an adapter-primer tagged with biotin. This result in a PCR product tagged with digoxigenin in one end and biotin in the other end, when both primers have been used to obtain the PCR product. This PCR product is divided into three aliquots. The first aliquot (C) is loaded untouched to the gel. The second aliquot (B) is mixed with Kilobase-Dynabeads (Invitrogen) coated with streptavidin. In case the PCR product is tagged with biotin, as an indication of the adapter primer having been involved in the PCR, the product will be withheld in the slothole as the beads will not be able to travel through the gel. The third aliquot (D) is mixed with Dynabeads (Invitrogen) coated with monoclonal anti-Digoxin antibodies (Sigma-Aldrich, Brøndby, Denmark). In case the PCR product is tagged with digoxigenin, as an indication of the teltail primer having been involved in the PCR, the product will be withheld in the slot-hole with the beads. (Separate experiments have shown that the beads do not retain untagged products in a manner which affects the experiment). As shown in these two examples (sample 1 and 2) all PCR products are withheld on both beads as an indication of both primers being involved in the PCR.

Method validation

Having designed Universal STELA to focus on the load of short telomeres, it was a challenge to find a suitable reference method for method validation. Among the available methods, we chose TRF and chromosome-specific STELA because they make use of the same material (DNA from a mixture of dividing and nondividing cells).

In a comparison of our results with the TRF assay, we had to obtain a mean measure from our Universal STELA data. This was performed by simply taking the mean length of all visible bands present. A comparison of Universal STELA mean (*Y*-axis) and TRF (*X*-axis) from a variety of cells with different telomere length is depicted in Fig. 3. It is here seen that the mean value obtained by Universal STELA is consistently lower than what is found with

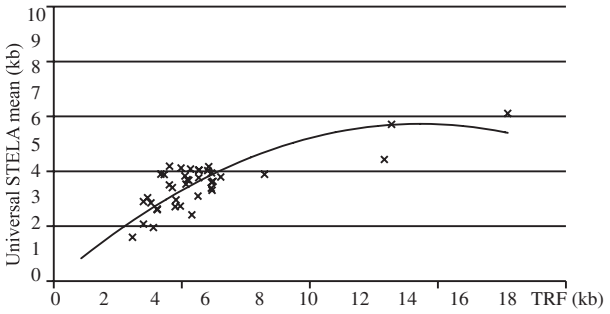

Fig. 3 The relationship between mean TRF length and mean length of visible bands obtained by Universal STELA. (Samples cover a wide variety of samples, including cell lines, fibroblasts and blood samples in order to cover the range between 3 and 18 kb.)

the TRF assay. We interpret this as caused by insufficient amplification of longer telomeric fragments (we obtain very few products above 8 kb) and preferential amplification of short telomeres in Universal STELA combined with TRF being insensitive to short telomeres. The overall conclusion of this comparison is therefore that Universal STELA is not suited for measuring mean telomeric length.

When comparing Universal STELA with XpYp STELA, it is a limitation that XpYp STELA measures only the telomeres from two single chromosome arms (in our case two Xp telomeres), while the Universal STELA has the potential to obtain length of telomeres from all chromosomes. Furthermore, mean telomere length values are biased by the fact that especially Universal STELA results in a truncated distribution of bands with only few bands longer than 8 Kb. In spite of these reservations, we did perform a comparison of the general length of visible bands obtained by the two methods at different PDs from the same fibroblast cell culture (Fig. 4A). In the comparison, we excluded samples with a mean value over 7 kb (as measured by TRF), and furthermore we chose to use median instead of mean, simply because the truncation mentioned earlier strongly suggests that the distribution of band length values is not a normal distribution. As seen in Fig. 4A, this comparison demonstrated that the length of bands obtained by Universal STELA is in general shorter than the length of bands obtained by Xp STELA. This finding can probably be explained by results of earlier work using metaphase FISH showing that Xp has mean telomere lengths that is longer than the mean length of all other chromosome ends taken together (Martens *et al.*, 1998) (Graakjaer *et al.*, 2003), but an element can still be that the PCR is being hampered to a higher degree in Universal STELA than in Xp STELA. We therefore also tried to compare only short bands between Xp STELA and Universal STELA. In this comparison, we found that the 5% shortest telomeres was consistently longer in Xp STELA than in Universal STELA (Fig. 4B). Because these very short telomeres are assumed to be created by a combination of replication driven and abrupt shortening caused by random DNA damage, their longer length in Xp STELA can probably not be fully explained by a general longer mean telomere length on Xp, but instead they may be longer because of special features of the X chromosome (X inactivation, replication timing), features that might interfere with sensitivity of the X chromosome to DNA damage. However, we are of the opinion that the results

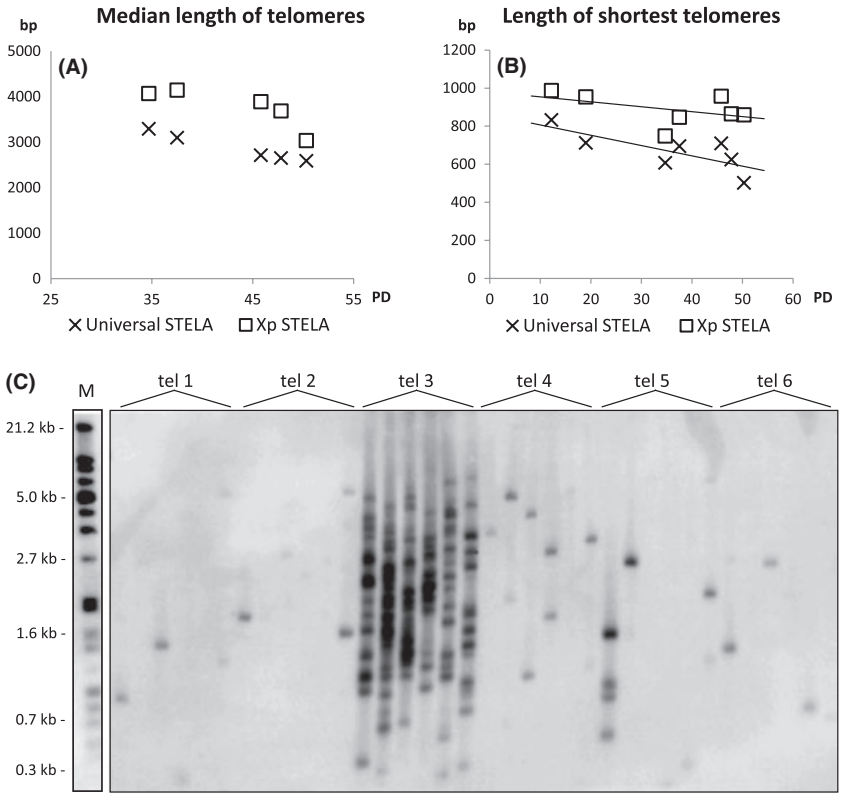

Fig. 4 Universal STELA compared to Xp STELA. (A) Median length of visible bands obtained by Xp STELA compared to Universal STELA from a normal fibroblast culture (only shown for PDs where the mean length by TRF was < 7 kb). (B) The mean length of the lowest 5% of telomeres obtained by Xp STELA compared to Universal STELA. (In the above comparisons the Xp products are corrected for the included non-telomeric fraction (344 bp), while Universal STELA products are only corrected for the included length derived from the panhandle oligos (42 bp)). (C) Universal STELA with the single telorettes. The second ligation step has been done with the six different telorettes ligated in separate tubes. (tel = telorette, for oligo sequences see Table 1).

in Fig. 4B indicate that the most dependable representation of all ultra-short telomeres in a sample will be obtained with Universal STELA.

As another comparison between the two methods, we have repeated an experiment earlier carried out by Sfeir *et al.* (2005). In this work, it was shown that the most proximal telomeric monomer on the 3'overhang in 80% of cases is GGTTAG by a specially designed telomere-end ligation protocol and confirmed by XpYp STELA. We repeated this finding with Universal STELA (Fig. 4C), confirming that Universal STELA has similar specificity for the telorette ligation as XpYp STELA.

Another validation approach is repeatability. By repeated measurements of the same DNA samples taken through, the whole Universal STELA procedure multiple times, we found a coefficient of variation (CV) of 0.10 for the number of bands below 1500 bp and 0.05 for mean length of all detected bands, indicating a reasonable good reproducibility of the Universal STELA method.

Results

In this section, we are presenting data from two sets of experiments, both aiming at correlating load of short telomeres as measured by Universal STELA to cell senescence. In the first part of this investigation, we wished to establish whether the amount of short telomeres changed with increasing population doublings as well as with the frequency of cells staining positive for β-Gal activity (SA-β-Gal staining), a marker associated with senescence. In the second part, we wished to explore whether the number of short telomeres is more abundant in senescent cells when compared to proliferating cells at the same passage, and whether senescent cells in early passages harbor as many short telomeres as senescent cells in late passages, thereby offering an explanation of premature cell senescence.

For these studies, we established two primary fibroblast cell lines and cultured these to senescence, harvesting DNA at regular intervals as well as staining for SA-β-Gal. In these culture experiments, we found a gradual, slow increase in SA-β-Gal-positive cells in cultures for the first 45 PDs followed by a sudden rapid increase in positive cells (Fig. 5A) correlating with cells obtaining typically senescent morphology.

While we found an expected gradual shortening of approximately 85 bp/PD in mean telomere length (Fig. 5B) for 50 PD's in both skin fibroblast cell lines when using TRF ($R^2 = 0.85$, $P < 0.001$), we found a gradual increase in the load of short telomeres in the first 40–45 PDs followed by an abrupt increase in the near-senescent PDs (Fig. 5C, D). When comparing the behavior of the number of short telomeres < 1500 bp pr genome equivalent in an increasingly old culture to the number of SA-β-Gal-positive cells in same PDs, it becomes apparent that there is a sudden, parallel increase in numbers seen with both parameters in late PDs. This is also reflected in a strong correlation between the two parameters, $R^2 = 0.93$ ($P < 0.001$) over 50 PD's. We performed the same analysis with Xp STELA and

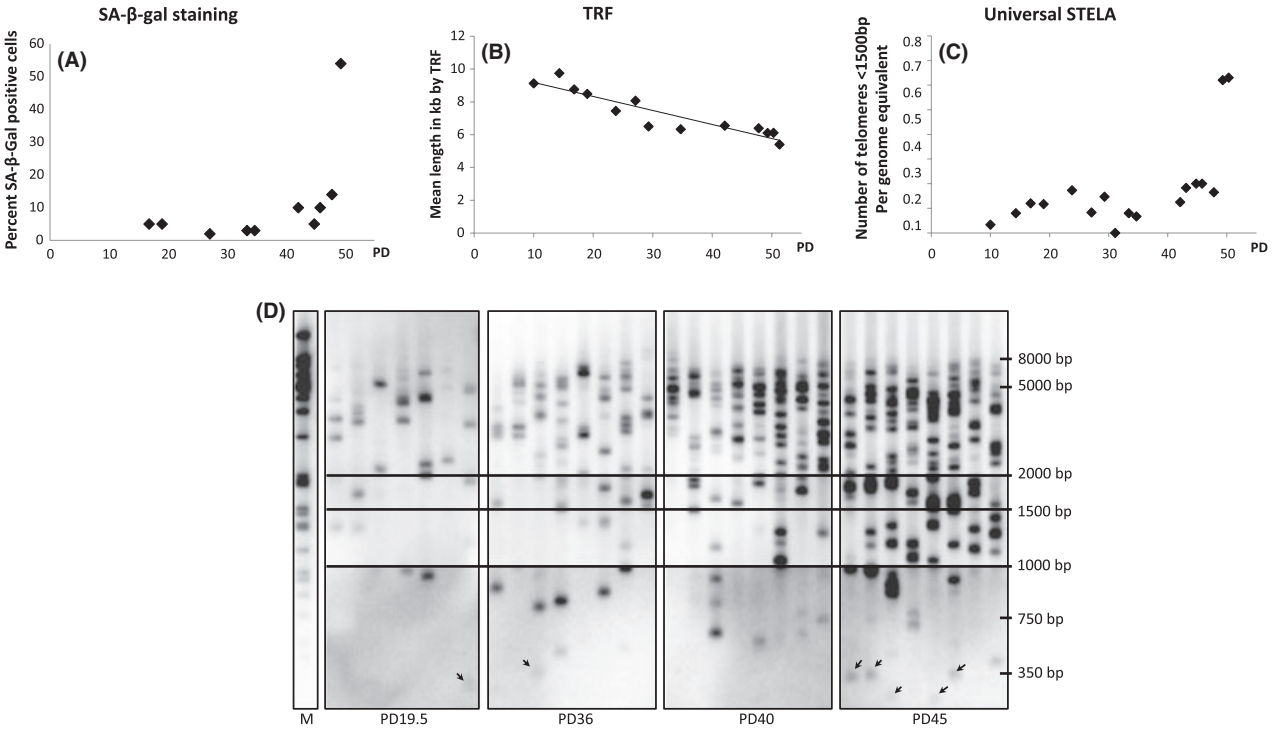

Fig. 5 Results from cell culture experiments. (A) The percentage of SA-β-Gal positive cells in increasing PDs for a primary skin fibroblast cell line showing an increase in late PD's. (B) The mean length of telomeres as analyzed by TRF in increasing PDs showing a gradual, linear decline of app. 85 bp/PD. (C) The load of short telomeres per genome equivalent in increasing PDs found by Universal STELA showing the same asynchronous increase in late PDs as the senescence marker. (D) Examples of results showing the increasing load of short telomeres in an increasing PD. It is seen that even very short telomeres (< 300 bp) are present in young as well as older cultures. (Arrows indicate ultra short telomeres).

tried to extract the number of short Xp telomeres per genome equivalent. The number of bands obtained with Xp STELA was, however, in general very low, and therefore firm conclusions are difficult to draw. But we saw no increase in number of bands as the culture approached senescence in this series, in contrast to our finding with Universal STELA (data not shown).

To be able to separate cells into cycling and noncycling subpopulations, we then stained growing cells with DiI. We found, as has previously been shown (Ferenac *et al.*, 2005), that DiI-stained fibroblasts do not exhibit any detectable changes in growth rate, morphology, or viability when compared with untreated cells. After culturing stained cells for 5–7 days, we found a bell-shaped distribution of fluorescence activity reflecting the difference in proliferation rates of different cells in the culture. We used FACS to isolate cells based on the DiI fluorescence assuming that the senescent (or noncycling) population stains more intensively using DiI (SEN) and the proliferating (or cycling) population stains less intensively using DiI (PROL), see Fig. 6A,B. Using this approach, we successfully sorted one fibroblast cell culture at three different passages (PD31.5, PD40, and PD47) as well as an MJ90 culture at a late passage (PD49.5).

When we examined the cell fractions in detail, we found that we had in fact isolated cells as a SEN population that morphologically had senescent characteristics, being larger and flatter. This was confirmed by SA-β-Gal staining, which showed that we had succeeded in enriching the SEN group more than threefold with SA-β-Gal-positive cells. Similarly, we obtained a PROL population almost depleted of SA-β-Gal-positive cells.

We then investigated purified DNA from corresponding PROL and SEN populations both for mean telomere length and for load of short telomeres. We performed TRF assays on all the samples from which we had obtained sufficient DNA to see whether we could find a difference in mean length in the sorted subpopulations as some authors had previously reported (Martin-Ruiz *et al.*, 2004). On the analyzed samples, we did not detect any differences in mean telomere length between the SEN and PROL subpopulations (data not shown).

When analyzing the load of short telomeres in the two subpopulations within the same PD, i.e. cells that have the same 'age', but show differences in proliferation capability, we found on average a 2.4-fold increase in the number of short telomeres per genome equivalent in the population enriched for nonproliferating cells (SEN) compared to the corresponding proliferating group (PROL) (Fig. 6C,D). It is seen that there is a wide variation in the observed numbers of short telomeres, but consistently we found more short telomeres in the senescent group compared to the proliferating group, although this was not significant

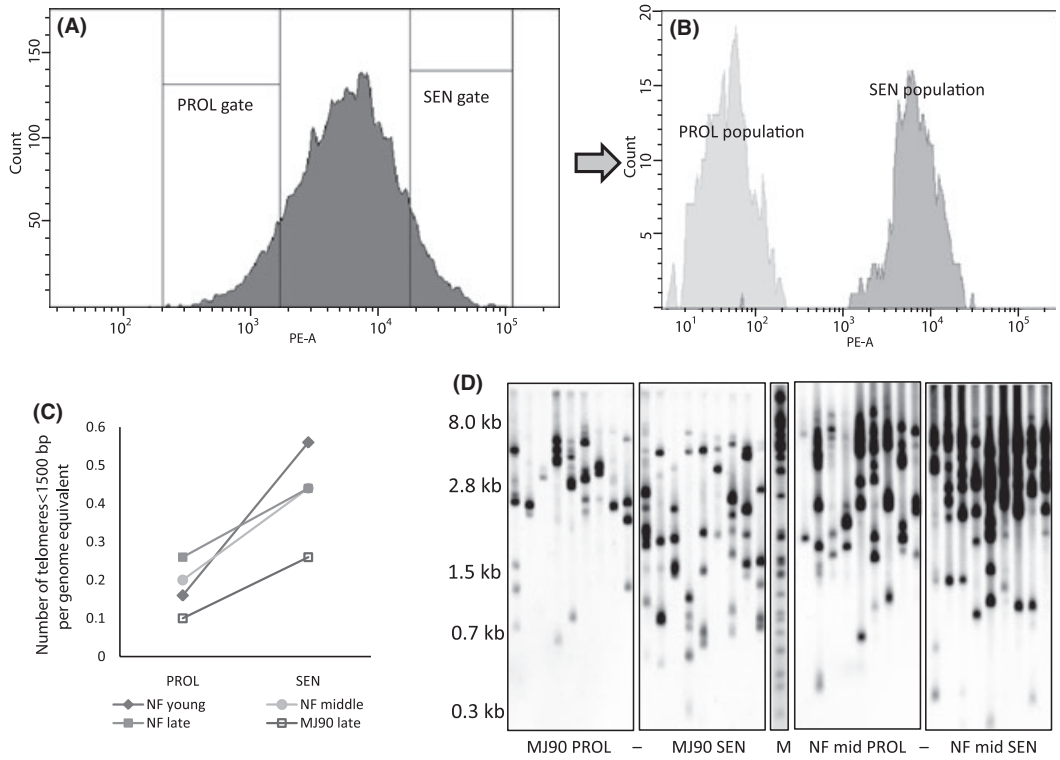

Fig. 6 Results from flowsort experiments. (A) Example of flowsort. After having cultured stained cells for 5–7 days a bell-shaped distribution of fluorescence activity reflecting the difference in number of cell division undergone in the culture is seen. Using this fluorescence signal as gating parameter an assumed senescent population with high DiI staining (SEN) and a proliferating population with low DiI staining (PROL) can be separated from the bulk of cells. (B) A control run of the two sorted populations showing that the PROL population has a low fluorescence staining, while the SEN population has a high degree of staining. (C) The load of short telomeres per genome equivalent obtained by Universal STELA in four different cell samples (NF young, middle and late and MJ90) flow sorted into two sub-populations: a cycling – proliferating population (PROL) and a non-cycling – senescent enriched population (SEN). It is seen how there is consistently more short telomeres in the SEN group than in the PROL group of the same cell sample. (D) Examples of Universal STELA results from the flowsort experiment.

using Wilcoxon matched-pairs signed-rank test ($P = 0.063$) because of only four samples being included in the comparison.

With regard to the length of the short telomeres, we found that in cultures where the mean telomere length over 20 passages fell from 9 kb to 5 kb all SEN populations had the 10 shortest telomeres at the same level, namely 200–1000 bp. In contrast, the telomere length values of the ten shortest bands in the PROL populations exhibited a decline in length with increasing passages corresponding to the decline in mean values but never reaching the same low level as the SEN group (data not shown).

Discussion

Shortening of telomeres has long been thought capable of inducing senescence. However, compelling evidence rejects the idea that an overall decline in length should be the direct inducer of senescence (Smith & Whitney, 1980; Rubelj & Vondracek, 1999; Martin-Ruiz *et al.*, 2004). Instead, emerging evidence suggests that shortening of a single or a few telomeres is a sufficient trigger (Abdallah *et al.*, 2009). However, many previous studies have had a methodological limit in demonstrating these short telomeres, because most methods measure either mean telomere length or telomere lengths of dividing and therefore nonsenescent cells. With Universal STELA, we have a tool that can directly investigate the relationship between senescence and the load of short telomeres on all cells in a population.

With this new method, we also present a new way of quantifying short telomeres. We suggest simply counting the number of short bands below a certain threshold and expressing this number relative to the DNA amount of one cell. Such a 'threshold' parameter seems a logical choice from a biological point of view, because it is a surrogate measure for the frequency within individual cells of telomeres that are no longer able to protect the chromosome ends. It is, however, not straightforward where to set such a threshold. To our knowledge, the field is still not certain as to how many telomere repeats are necessary to form the protective cap on the chromosome ends. It has been shown that cancer cells harbor t-stumps of only a few repeats (Xu & Blackburn, 2007), but this cannot assist us in setting a 'normal' threshold. It has also been shown that old cell cultures harbor very short telomeres (Baird *et al.*, 2003), but yet again these could have been harvested from senescent cells where the telomeres are 'too short' and already have triggered the cells' senescence mechanisms.

In this study, we have suggested to set the threshold at 1500 bp and by using this threshold found a strong correlation with SA-β-Gal staining. We have found similarly good correlations when lowering the threshold to 1000 bp. However, when the threshold is set too low, the contribution of the stochastic variation becomes high, because the number of short telomeres becomes very low. Increasing the threshold to 2000 bp also gives good correlations, but we have seen that in older cells telomeres just around 2000 bp can be quite common. We believe this is attributed to the gradual replicative shortening of telomeres slowly beginning to reach this length. Even though we acknowledge the increasing influence on mean telomere length when the cells approach senescence, we find that setting the threshold too high will make the method less sensitive to the more abrupt changes. (It must be noted that in a product of 1500 bp, the annealed oligos contribute with approximately 70 bp and the subtelomeric region with, on average, 300 bp). Here, it should be pointed out that the choice of threshold was based on data obtained from skin fibroblasts. Considering the mechanisms protecting the telomeres (shelterin complex, t-loop), it seems likely that the fragment of telomere sequence needed for protection should be rather similar between cell types. However, one thing that might influence the threshold is telomerase activity in the cell, because it has been suggested that telomerase, in addition to elongating the telomeres, also stabilizes the telomeres (Blackburn, 2001; Sharma *et al.*, 2003; Bollmann, 2008).

As mentioned, the number of bands below the threshold is expressed per genome equivalent. It should here be stressed that the number of bands per genome equivalent is a minimum estimate, because the calculation assumes 100% recovery through digestion, ligation, and PCR. This is most likely not the case, but the error imposed by this assumption is believed to be constant. This assumption is supported by our method reproducibility and also by our findings in the culture experiments presented in the results section, where we demonstrated the applicability of this new measure. Despite a gradual decrease in mean length measured by TRF, we found an asynchronous, rapid increase in the number of short telomeres in near-senescent cell cultures. The load of short telomeres correlated strongly with SA-β-Gal staining, which is suggestive of a causal relationship but does not rule out the possibility that they could be independent markers of an unidentified senescence mechanism. Our indications of a lack of increase in short bands from Xp when cells are approaching senescence is surprising considering the current believe that all telomere ends can induce senescence. We cannot rule out that it can be attributed to methodological limitations (XpYp STELA is maybe not suitable for extracting a load measure) but note that others before us also have found that XpYp telomeres can be rather long and with very few ultrashort telomeres in senescent primary skin fibroblast cell cultures like the one we report from here (see e.g. Baird *et al.*, 2003).We cannot immediately explain the apparent discrepancy between Xp telomeres and the mixed population of telomeres, but if it is true, we can only speculate whether it has to do with special features of the X chromosome as mentioned earlier (replication timing, X inactivation). Further studies are needed to clarify whether this is a general finding or whether it is tissue-, clone- or maybe even donor specific.

To further elucidate on the correlation between load of short telomeres and senescence, we performed the flow sorting experiment, achieving enrichment of cell populations with either senescent or proliferating cells. We found a marked difference in the number of short telomeres between the senescent subpopulation and the proliferating subpopulation, together

with a tendency that the lengths of short telomeres were similar in senescent cells independent of the number of population doublings. Our results are thus consistent with earlier findings by the von Zglinicki group (Martin-Ruiz *et al.*, 2004).

We find no difference in mean length, but a marked (although not significant) difference in the load of short telomeres between the senescent and proliferative subpopulations. Although we cannot exclude the possibility that the short telomeres are found within a few cells that have cycled more rapidly than the rest, these results support the hypothesis that besides gradual telomere loss, some other telomeric shortening mechanism contributes significantly to causing cells to enter senescence.

A mechanism causing such telomeric damage can be assumed to be coupled to the asynchronous way that cells enter senescence. Oxidative damage of telomeres along with a general damage of DNA because of aged and thereby inefficient mitochondria could be an explanation (Chen *et al.*, 1995), although contradictory results have been published on this matter (von Zglinicki *et al.*, 2000; Britt-Compton *et al.*, 2009). The existence of such a shortening mechanism is also supported by our previously published finding that even telomerase-immortalized hMSC cells with a mean telomere length around 18 kb contain a few very short telomeres (below 1500 bp) (Christensen *et al.*, 2008).

Based on extrapolations from load of short telomeres to number of short telomeres per cell, and keeping in mind that probably not all short telomeres in a sample result in visible bands (see above), it seems that each cell only needs to harbor one or a few ultra-short telomeres to activate the senescent pathway. It should in this connection be pointed out that the number of short telomeres per genome equivalent is very low compared to all telomeres in the cell, also in senescent cells, which could explain why we see no difference in mean telomere length between PROL- and SEN-derived DNA.

Universal STELA is based on the original STELA method but has been adapted, so that a 'load of short telomeres' can be derived. This measure can be considered meaningful in the Universal STELA method because we cover most chromosomes but less logical in XpYp STELA where only telomeres from X and Y chromosomes are being measured.

This approach is at the expense of information on what chromosome arms the shortest telomeres are located. This limitation is, however, not expected to be a major problem, because it is generally believed that any chromosome carrying an ultra-short telomere can be the cause of senescence in a cell. This, however, does not exclude that certain chromosome ends will be less commonly causing senescence, because they have in general longer telomeres than average (Graakjaer *et al.*, 2003). We believe that in most (clinical) situations, it is not of importance to know which chromosome arm is the shortest, but that it is of absolute importance to know the load of the shortest telomeres. For research purposes, it could, however, sometimes be interesting to gain information also on specific chromosomes. We have obtained preliminary data suggesting that this can be performed by designing subtelomeric specific probes for selected chromosomes and use these probes for detection in combination with the telomeric probe in Universal STELA.

A major obstacle to Universal STELA seems to be the small yet unknown subtelomeric parts remaining in the products, as we know it from the TRF assay. We have designed the method to ensure that most of the subtelomeric region is removed by digestion. There are certain problems when doing this. Firstly, not all subtelomeric regions have been sequenced yet, and secondly, we do not know to what extent the telomere-near sites are accessible for digestion (Steinert *et al.*, 2004). The problem is, however, diminished by the way we analyze our data, although we will underestimate the number of short telomeres to a certain degree, because we lose information from a few chromosomes with only a relevant restriction site far from the telomeric repeat (e.g. 10q and 21q). Our attempt to trim the subtelomeric region gives rise to the possibility that we cut within the most centromeric part of the telomere where the variant repeats are common because we have chosen MseI as our primary cutter. We do however believe this to be a minor concern, firstly because the variant TTAAGGG seems to occur infrequently, and secondly because regions with such variant repeats are most likely not functioning as true telomeres because of the fact that the proteins of the shelterin complex are in general believed to show sequence specificity to (TTAGGG)n repeats (Zhong *et al.*, 1992; de Lange, 2005). In any case, these problems will be of minor importance in many types of applications, e.g. when studying the same cell line under different conditions (as in the reported study), thus registering relative changes in telomere length. This will often be the case in clinical settings e.g. when treating patients with drugs targeting the telomere maintenance system, where one would aim at detecting changes within a patient.

Universal STELA is not a suitable method for measuring mean telomere length as clearly shown in this study (Fig. 3), and therefore it should be used only where investigators are interested in studying the distribution and load of the shorter telomeres. The limitation could perhaps be overcome by improving the PCR conditions, but this would be a very laborious way to achieve a mean, and therefore other methods would be preferable. As the method is laborious, it is also less suited for large-scale epidemiological studies. This is also true for the conventional STELA, and the work load for the two methods must be considered equal, because we have only added a simple ligation step, and because both methods rely on the Southern blotting technique.

An obvious advantage of both STELA versions is that they work with very little DNA as template. Therefore, it will be possible to work on scarce patient material as well as sorted or dissected cells that are often very limited in number. The amount of DNA used for STELA is at a range where DNA purification steps will most often be the limiting step. Further, the purification step is important because both STELA methods require good quality DNA. In situations where only archival or paraffin-embedded tissue is available, other methods must be chosen, e.g. Q-FISH.

The main advantage of Universal STELA is that it is the first method that can estimate the load of short telomeres regardless of chromosome and from samples containing nondividing cells. With the existing methods, it has been possible to measure short telomeres, but not as universally as with our new method. While Q-FISH analysis of metaphases can give important information on the length of telomeres on specific chromosomes, the method is limited to dividing cells. TRF and Q-FISH assays can to a certain degree show the distribution of telomere length. TRF is, however, insensitive to the shortest telomeres, and the Q-FISH-based methods only give a mean length. While the original chromosome-specific STELA has taught us that there is an extensive variation in the length of individual telomeres, any conclusion based on this method will have to be considered with some reservation, because it is not certain that the findings are representative. One could argue that if the same findings were true for two or more different telomeres then it might be sufficient evidence for a generalization, but in that case it would be more feasible to run Universal STELA. Furthermore, this study comparing Xp STELA and Universal STELA suggests that in some situations biologically relevant changes in load of short telomeres may be missed if focusing only on a single chromosome arm.

This new method, Universal STELA, therefore offers some advantages compared to existing methods and can be used to explore many of the unanswered questions in telomere biology including the role that telomeres play in cancer and aging.

Material and method

Cell culture

Two primary skin fibroblast cultures were established from healthy women undergoing operation for breast reduction after we had obtained their informed consent (NF66 and NF83). A late MJ90 culture was kindly supplied by IR. All cells were cultured in DMEM (Invitrogen, Taastrup, Denmark) supplemented with 10% BSA. Cells were passaged when 80–90% confluent. We cultured one cell line (NF83) until it reached senescence, harvesting cells for SA-β-gal staining and DNA weekly. From the other cell line (NF66), ampules were frozen at four different passages (corresponding to PD 19.5, PD 27, PD 36, and PD 44) and used for flow sorting, before continuing growth to senescence.

DNA extraction

DNA was extracted using the common high-salt method (modified from Aljanabi and Martinez, 1997). Concentration and purity were evaluated on a Nanodrop (Thermo Scientific).

TRF assay

For the TRF assay-based determination of telomere length, the TeloTAGGG telomere length assay from Roche was used according to the manufacturer's manual with few adaptations. In principle, 0.5–1 μg of isolated DNA was digested either by HinfI/RsaI (Roche), MseI/NdeI, or HphI/MnlI (NEB). HinfI and RsaI are known to cut outside the subtelomeric region, NdeI recognizes the sequence CATATG while HphI, MnlI, and MseI recognize the supposed telomere repeat variants GGTGA, GAGG, and TTAA respectively.

The digested DNA was separated by gel electrophoresis on a 0.75% TBE Seakem agarose gel and transferred to a nylon membrane by Southern blotting using a vacuum blotter. The blotted DNA fragments were then hybridized overnight to a digoxigenin (DIG)-labeled probe, specific for the telomeric sequence, and subsequently incubated with a DIG-specific antibody coupled with alkaline phosphate. Finally, the telomere probe was visualized using a chemiluminescent substrate (CDP-Star), and the chemiluminescence signal was detected using a BioImager from UVP. The TRF lengths were calculated using VISION WORKS software from UVP (Upland, CA, USA).

XpYp STELA

XpYp STELA was adapted from Sfeir *et al.* (2005). Isolated DNA was digested by EcoRI, quantified by Picogreen (Invitrogen) or on a Nanodrop and diluted if necessary. To 10 ng of digested DNA, 20 U of T4DNA ligase, 10^{-3} μM telorette, 1× NEBuffer2, and 1× ATP were added in a 15 μL volume and left overnight at 35 °C followed by a 20-min inactivation step of 65 °C. DNA was diluted to 250 pg μL^{-1} with water.

Multiple PCRs were carried out for each sample in a 12 μL volume containing 200–500 pg of ligated DNA, 1× Failsafe PCR PreMix H (Epicentre, Madison, WI, USA), 0.1 μM teltail and XpYpE2 primers, and 1.25 U of Failsafe enzyme (Epicentre). The reaction was carried out on a Hybaid Thermocycler (Thermo Electron, Waltham, MA, USA) under the following conditions: 1 cycle of 95 °C for 2 min, 26 cycles of 95 °C for 15 s, 58 °C for 30 s and 72 °C for 10 min, 1 cycle of 72 °C for 15 min. (For oligo and primer sequences see Table 1).

Detection of the PCR products was carried out as described for the TRF assay except that the gel was a 0.85% agarose to separate the shorter bands better. The size of the PCR products was calculated on the basis of the molecular weight marker (Roche, Hvidovre, Denmark) using VISIONWORKS Software from UVP.

Universal STELA

Isolated DNA was digested by a 1:1 mixture of MseI and NdeI. Ten nanograms of digested DNA was mixed with 50 μmol 42-mer and 50 μmol 11 + 2-mer in a 7 μL volume. (For oligo and primer sequences see Table 1). The mixture was ramped down from 65 °C to 16 °C over 1 h. Twenty units T4 DNA ligase (NEB) was then quickly added together with 1× NEBuffer2 and 1×ATP and left overnight at 16 °C. Additionally, 20 U of T4DNA ligase and 10^{-3} μM telorette were added, and the reaction mixture was supplemented to 1× NEBuffer2 and 1× ATP in a 25 μL volume and left overnight at 35 °C followed by a 20-min

inactivation step of 65 °C. These procedures can be performed in one tube with no intermediate purification steps.

PCR was carried out in a 12 μL volume containing 20–50 pg of ligated DNA, 1× Failsafe PCR PreMix H (Epicentre), 0.1 μM telt-ail and Adapter primers, and 1.25 U of Failsafe enzyme (Epicentre). The reaction was carried out on a Hybaid Thermocycler (Thermo Electron) under the following conditions: 1 cycle of 68 °C for 5 min, 1 cycle of 95 °C for 2 min, 26 cycles of 95 °C for 15 s, 58 °C for 30 s and 72 °C for 12 min, 1 cycle of 72 °C for 15 min. The initial step of 68C was the fill-in step.

Detection of telomere repeat fragments was carried out by Southern technique as described for XpYp STELA, using a (TTAGGG)n – DIG-labeled probe.

β-Gal staining

Cells were seeded in slide flasks, washed twice in PBS, and fixed for 5 min at room temperature in 3.7% formaldehyde. After washing, the cells were incubated at 37 °C (no CO_2) over night with fresh β-gal solution containing 1 mg of 5-bromo-4-chloro-3-indolyl β-D-galactoside (X-Gal; Sigma-Aldrich, Brøndby, Denmark) per mL, 40 mM citric acid (pH 6.0), 5 mM potassium ferrocyanide, 5 mM potassium ferricyanide, 150 mM NaCl, and 2 mM $MgCl_2$. From each slide flask, a minimum of 200 cells was counted under the microscope.

DiI staining

Cells were trypsinized and stained in suspension for 20 min in 5 μM solution of DiI (catalog No. D282, 100 mg; Molecular Probes, Eugene, OR, USA), washed twice, seeded in culture flasks at approximately 2.000 cells cm^{-2}, and cultured in the dark. After 5–7 days, cells were trypsinized, washed twice in freshly prepared PBS containing 2% FBS and 0.02% EDTA, and resuspended in the same buffer. Control cells were seeded under same conditions with the exception that they were not stained. At the day of the experiment, control cells were trypsinized. Negative controls were simply washed, while positive control cells were stained for 20 min with DiI and then washed and resuspended in the same buffer as the sample cells. All cells were kept on ice until sorting.

Flow sorting

Cells were analyzed and sorted on a BD FACSAria I Cell-Sorting System (BD Bioscience, Brøndby, Denmark) equipped with a blue 488-nm Coherent® SapphireTM solid state (13–20 mW) and a red 633-nm JDS Uniphase™ HeNe (10–20 mW) laser (JDS Uniphase Corp., Milpitas, CA, USA). Forward-scattered light and side-scattered light were detected with linear signal amplification (Photodiode detector with a 488/10 bandpass filter and photomultiplier tube with 488/10 bandpass, respectively), whereas DiI-specific fluorescence emission was detected by a photomultiplier tube with a 585/42 bandpass filter and logarithmic signal amplification. Two cell populations with high (SEN) and low (PROL) DiI stain were sorted simultaneously into 5-mL Falcon tubes containing 1 mL of FBS. Standard purity mode was used. Collected cells were resuspended in PBS buffer and used for DNA isolation and SA-ß-gal staining.

Statistics

Linear regression analysis, Wilcoxon matched-pairs signed-rank test and Mann–Whitney two-sample rank-sum test were carried out in STATA/SE9.

Acknowledgments

The authors thank Maria Harbo, Nedime Serakinci, and Lene Byriel for their assistance and for fruitful discussions and Marianne Hansen for technical assistance. LB was supported by a PhD scholarship provided by Vejle Hospital, University of Southern Denmark and the Danish Aging Research Center.

Author contributions

SK and LB have both contributed to the ideas, designing, and planning of Universal STELA and are the sole inventors of this method. IR, PBH, and UBJ assisted in planning and carrying out the flow sort experiment. The acquisition of data was carried out by LB, while analysis and interpretation was carried out by LB and SK. Results were discussed with IR, PBH, and UBJ. LB and SK both contributed equally to the manuscript, while IR, PBH, and UBJ only contributed to the parts concerning flow sorting data. All have approved the final manuscript.

References

Abdallah P., Luciano P., Runge K.W., Lisby M., Geli V., Gilson E., Teixeira M.T. (2009) A two-step model for senescence triggered by a single critically short telomere. *Nat. Cell Biol.* **11**, 988–993.

d'Adda di Fagagna F., Reaper P.M., Clay-Farrace L., Fiegler H., Carr P., Von Zglinicki T., Saretzki G., Carter N.P., Jackson S.P. (2003) A DNA damage checkpoint response in telomere-initiated senescence. *Nature* **426**, 194–198.

Aljanabi S.M., Martinez I. (1997) Universal and rapid salt-extraction of high quality genomic DNA for PCR-based technqiues. *Nucleic Acids Res* **25**, 4692–4693.

Allshire R.C., Dempster M., Hastie N.D. (1989) Human telomeres contain at least three types of G-rich repeat distributed non-randomly. *Nucleic Acids Res.* **17**, 4611–4627.

Allsopp R.C., Harley C.B. (1995) Evidence for a critical telomere length in senescent human fibroblasts. *Exp. Cell Res.* **219**, 130–136.

Allsopp R.C., Vaziri H., Patterson C., Goldstein S., Younglai E.V., Futcher A.B., Greider C.W., Harley C.B. (1992) Telomere length predicts replicative capacity of human fibroblasts. *Proc. Natl. Acad. Sci. U S A* **89**, 10114–10118.

Allsopp R.C., Chang E., Kashefi-Aazam M., Rogaev E.I., Piatyszek M.A., Shay J.W., Harley C.B. (1995) Telomere shortening is associated with cell division in vitro and in vivo. *Exp. Cell Res.* **220**, 194–200.

Alter B.P., Baerlocher G.M., Savage S.A., Chanock S.J., Weksler B.B., Willner J.P., Peters J.A., Giri N., Lansdorp P.M. (2007) Very short

telomere length by flow fluorescence in situ hybridization identifies patients with dyskeratosis congenita. *Blood* **110**, 1439–1447.

Baird D.M. (2008) Mechanisms of telomeric instability. *Cytogenet. Genome Res.* **122**, 308–314.

Baird D.M., Jeffreys A.J., Royle N.J. (1995) Mechanisms underlying telomere repeat turnover, revealed by hypervariable variant repeat distribution patterns in the human Xp/Yp telomere. *EMBO J.* **14**, 5433–5443.

Baird D.M., Rowson J., Wynford-Thomas D., Kipling D. (2003) Extensive allelic variation and ultrashort telomeres in senescent human cells. *Nat. Genet.* **33**, 203–207.

Baird D.M., Britt-Compton B., Rowson J., Amso N.N., Gregory L., Kipling D. (2006) Telomere instability in the male germline. *Hum. Mol. Genet.* **15**, 45–51.

Bischoff C., Graakjaer J., Petersen H.C., Jeune B., Bohr V.A., Koelvraa S., Christensen K. (2005) Telomere length among the elderly and oldest-old. *Twin. Res. Hum. Genet.* **8**, 425–432.

Blackburn E.H. (2001) Switching and signaling at the telomere. *Cell* **106**, 661–673.

Bodnar A.G., Ouellette M., Frolkis M., Holt S.E., Chiu C.P., Morin G.B., Harley C.B., Shay J.W., Lichtsteiner S., Wright W.E. (1998) Extension of life-span by introduction of telomerase into normal human cells. *Science* **279**, 349–352.

Bollmann F.M. (2008) The many faces of telomerase: emerging extratelomeric effects. *Bioessays* **30**, 728–732.

Britt-Compton B., Rowson J., Locke M., Mackenzie I., Kipling D., Baird D.M. (2006) Structural stability and chromosome-specific telomere length is governed by cis-acting determinants in humans. *Hum. Mol. Genet.* **15**, 725–733.

Britt-Compton B., Wyllie F., Rowson J., Capper R., Jones R.E., Baird D.M. (2009). Telomere dynamics during replicative senescence are not directly modulated by conditions of oxidative stress in IMR90 fibroblast cells. *Biogerontology*. **10**, 683–693.

Canela A., Vera E., Klatt P., Blasco M.A. (2007) High-throughput telomere length quantification by FISH and its application to human population studies. *Proc. Natl. Acad. Sci. U S A* **104**, 5300–5305.

Chen Q., Fischer A., Reagan J.D., Yan L.J., Ames B.N. (1995) Oxidative DNA damage and senescence of human diploid fibroblast cells. *Proc. Natl. Acad. Sci. U S A* **92**, 4337–4341.

Christensen R., Alsner J., Brandt S.F., Dagnaes-Hansen F., Kolvraa S., Serakinci N. (2008) Transformation of human mesenchymal stem cells in radiation carcinogenesis: long-term effect of ionizing radiation. *Regen. Med.* **3**, 849–861.

Counter C.M., Avilion A.A., LeFeuvre C.E., Stewart N.G., Greider C.W., Harley C.B., Bacchetti S. (1992) Telomere shortening associated with chromosome instability is arrested in immortal cells which express telomerase activity. *EMBO J.* **11**, 1921–1929.

Ferenac M., Polancec D., Huzak M., Pereira-Smith O.M., Rubelj I. (2005) Early-senescing human skin fibroblasts do not demonstrate accelerated telomere shortening. *J. Gerontol. A Biol. Sci. Med. Sci.* **60**, 820–829.

Graakjaer J., Bischoff C., Korsholm L., Holstebroe S., Vach W., Bohr V.A., Christensen K., Kolvraa S. (2003) The pattern of chromosome-specific variations in telomere length in humans is determined by inherited, telomere-near factors and is maintained throughout life. *Mech. Ageing Dev.* **124**, 629–640.

Harley C.B., Futcher A.B., Greider C.W. (1990) Telomeres shorten during ageing of human fibroblasts. *Nature* **345**, 458–460.

Hastie N.D., Dempster M., Dunlop M.G., Thompson A.M., Green D.K., Allshire R.C. (1990) Telomere reduction in human colorectal carcinoma and with ageing. *Nature* **346**, 866–868.

Hemann M.T., Strong M.A., Hao L.Y., Greider C.W. (2001) The shortest telomere, not average telomere length, is critical for cell viability and chromosome stability. *Cell* **107**, 67–77.

Henderson S., Allsopp R., Spector D., Wang S.S., Harley C. (1996) In situ analysis of changes in telomere size during replicative aging and cell transformation. *J. Cell Biol.* **134**, 1–12.

Kimura M., Cherkas L.F., Kato B.S., Demissie S., Hjelmborg J.B., Brimacombe M., Cupples A., Hunkin J.L., Gardner J.P., Lu X., Cao X., Sastrasinh M., Province M.A., Hunt S.C., Christensen K., Levy D., Spector T.D., Aviv A. (2008a) Offspring's leukocyte telomere length, paternal age, and telomere elongation in sperm. *PLoS Genet.* **4**, e37.

Kimura M., Hjelmborg J.V., Gardner J.P., Bathum L., Brimacombe M., Lu X., Christiansen L., Vaupel J.W., Aviv A., Christensen K. (2008b) Telomere length and mortality: a study of leukocytes in elderly Danish twins. *Am. J. Epidemiol.* **167**, 799–806.

de Lange T. (2005) Shelterin: the protein complex that shapes and safeguards human telomeres. *Genes Dev.* **19**, 2100–2110.

Lansdorp P.M., Verwoerd N.P., van de Rijke F.M., Dragowska V., Little M.T., Dirks R.W., Raap A.K., Tanke H.J. (1996) Heterogeneity in telomere length of human chromosomes. *Hum. Mol. Genet.* **5**, 685–691.

Lavrentieva I., Broude N.E., Lebedev Y., Gottesman I.I., Lukyanov S.A., Smith C.L., Sverdlov E.D. (1999) High polymorphism level of genomic sequences flanking insertion sites of human endogenous retroviral long terminal repeats. *FEBS Lett.* **443**, 341–347.

Levy M.Z., Allsopp R.C., Futcher A.B., Greider C.W., Harley C.B. (1992) Telomere end-replication problem and cell aging. *J. Mol. Biol.* **225**, 951–960.

Lindsey J., McGill N.I., Lindsey L.A., Green D.K., Cooke H.J. (1991) In vivo loss of telomeric repeats with age in humans. *Mutat. Res.* **256**, 45–48.

Martens U.M., Zijlmans J.M., Poon S.S., Dragowska W., Yui J., Chavez E.A., Ward R.K., Lansdorp P.M. (1998) Short telomeres on human chromosome 17p. *Nat. Genet.* **18**, 76–80.

Martens U.M., Chavez E.A., Poon S.S., Schmoor C., Lansdorp P.M. (2000) Accumulation of short telomeres in human fibroblasts prior to replicative senescence. *Exp. Cell Res.* **256**, 291–299.

Martin-Ruiz C., Saretzki G., Petrie J., Ladhoff J., Jeyapalan J., Wei W., Sedivy J., von Z.T. (2004) Stochastic variation in telomere shortening rate causes heterogeneity of human fibroblast replicative life span. *J. Biol. Chem.* **279**, 17826–17833.

Olovnikov A.M. (1973) A theory of marginotomy. The incomplete copying of template margin in enzymic synthesis of polynucleotides and biological significance of the phenomenon. *J. Theor. Biol.* **41**, 181–190.

O'Sullivan J.N., Finley J.C., Risques R.A., Shen W.T., Gollahon K.A., Moskovitz A.H., Gryaznov S., Harley C.B., Rabinovitch P.S. (2004) Telomere length assessment in tissue sections by quantitative FISH: image analysis algorithms. *Cytometry A* **58**, 120–131.

Parrinello S., Samper E., Krtolica A., Goldstein J., Melov S., Campisi J. (2003) Oxygen sensitivity severely limits the replicative lifespan of murine fibroblasts. *Nat. Cell Biol.* **5**, 741–747.

Passos J.F., Von Zglinicki T. (2006) Oxygen free radicals in cell senescence: are they signal transducers? *Free Radic. Res.* **40**, 1277–1283.

Passos J.F., Saretzki G., von Z.T. (2007) DNA damage in telomeres and mitochondria during cellular senescence: is there a connection? *Nucleic Acids Res.* **35**, 7505–7513.

Richter T., von Z.T. (2007) A continuous correlation between oxidative stress and telomere shortening in fibroblasts. *Exp. Gerontol.* **42**, 1039–1042.

Riethman H. (2008) Human telomere structure and biology. *Annu. Rev. Genomics Hum. Genet.* **9**, 1–19.

Rubelj I., Vondracek Z. (1999) Stochastic mechanism of cellular aging–abrupt telomere shortening as a model for stochastic nature of cellular aging. *J. Theor. Biol.* **197**, 425–438.

Rubelj I., Huzak M., Brdar B., Pereira-Smith O.M. (2002) A single-stage mechanism controls replicative senescence through Sudden Senescence Syndrome. *Biogerontology* **3**, 213–222.

Rufer N., Dragowska W., Thornbury G., Roosnek E., Lansdorp P.M. (1998) Telomere length dynamics in human lymphocyte subpopulations measured by flow cytometry. *Nat. Biotechnol.* **16**, 743–747.

Sfeir A.J., Chai W., Shay J.W., Wright W.E. (2005) Telomere-end processing the terminal nucleotides of human chromosomes. *Mol. Cell* **18**, 131–138.

Sharma G.G., Gupta A., Wang H., Scherthan H., Dhar S., Gandhi V., Iliakis G., Shay J.W., Young C.S., Pandita T.K. (2003) hTERT associates with human telomeres and enhances genomic stability and DNA repair. *Oncogene* **22**, 131–146.

Sherr C.J., DePinho R.A. (2000) Cellular senescence: mitotic clock or culture shock? *Cell* **102**, 407–410.

Smith J.R., Whitney R.G. (1980) Intraclonal variation in proliferative potential of human diploid fibroblasts: stochastic mechanism for cellular aging. *Science* **207**, 82–84.

Steinert S., Shay J.W., Wright W.E. (2004) Modification of subtelomeric DNA. *Mol. Cell. Biol.* **24**, 4571–4580.

Vaziri H., Dragowska W., Allsopp R.C., Thomas T.E., Harley C.B., Lansdorp P.M. (1994) Evidence for a mitotic clock in human hematopoietic stem cells: loss of telomeric DNA with age. *Proc. Natl. Acad. Sci. U S A* **91**, 9857–9860.

Von Zglinicki T., Saretzki G., Docke W., Lotze C. (1995) Mild hyperoxia shortens telomeres and inhibits proliferation of fibroblasts: a model for senescence? *Exp. Cell Res.* **220**, 186–193.

Wang R.C., Smogorzewska A., deLange T. (2004) Homologous recombination generates T-loop-sized deletions at human telomeres. *Cell* **119**, 355–368.

Xu L., Blackburn E.H. (2007) Human cancer cells harbor T-stumps, a distinct class of extremely short telomeres. *Mol. Cell* **28**, 315–327.

von Zglinicki T., Pilger R., Sitte N. (2000) Accumulation of single-strand breaks is the major cause of telomere shortening in human fibroblasts. *Free Radic. Biol. Med.* **28**, 64–74.

Zhong Z., Shiue L., Kaplan S., de L.T. (1992) A mammalian factor that binds telomeric TTAGGG repeats in vitro. *Mol. Cell. Biol.* **12**, 4834–4843.

Zou Y., Sfeir A., Gryaznov S.M., Shay J.W., Wright W.E. (2004) Does a sentinel or a subset of short telomeres determine replicative senescence? *Mol. Biol. Cell* **15**, 3709–3718.